Invest New Drugs
DOI 10.1007/s10637-017-0494-4

PRECLINICAL STUDIES

Anti-invasive effects of CXCR4 and FAK inhibitors in non-small cell lung carcinomas with mutually inactivated p53 and PTEN tumor suppressors

Miodrag Dragoj[1] · Jasna Bankovic[1] · Evangelia Sereti[2] · Sofija Jovanovic Stojanov[1] · Konstantinos Dimas[2] · Milica Pesic[1] · Tijana Stankovic[1]

Received: 10 May 2017 / Accepted: 13 July 2017

Summary Non-small cell lung carcinoma (NSCLC) is the most common type of lung cancer. At the time of diagnosis, a large percentage of NSCLC patients have already developed metastasis, responsible for extremely high mortality rates. CXCR4 receptor and focal adhesion kinase (FAK) are known to regulate such invasive cancer behavior. Their expression is downregulated by p53 and PTEN tumor suppressors which are commonly co-inactivated in NSCLC patients and contribute to metastasis. Therefore, targeting CXCR4 or FAK seems to be a promising strategy in suppressing metastatic spread of p53/PTEN deficient NSCLCs. In this study, we first examined the invasive characteristics of NSCLC cells with suppressed p53 and PTEN activity using wound healing, gelatin degradation and invasion assays. Further, changes in the expression of CXCR4 and FAK were evaluated by RT-qPCR and Western Blot analysis. Finally, we tested the ability of CXCR4 and FAK inhibitors (WZ811 and PF-573228, respectively) to suppress the migratory and invasive potential of p53/PTEN deficient NSCLC cells, in vitro and in vivo using metastatic models of human NSCLC. Our results showed that cells with mutually inactive p53 and PTEN have significantly increased invasive potential associated with hyperactivation of CXCR4 and FAK signaling pathways. Treatments with WZ811 and PF-573228 inhibitors significantly reduced migratory and invasive capacity in vitro and showed a trend of improved survival in vivo. Accordingly, we demonstrated that p53/PTEN deficient NSCLCs have extremely invasive phenotype and provided a rationale for the use of CXCR4 or FAK inhibitors for the suppression of NSCLC dissemination.

Keywords CXCR4 · FAK · PTEN · p53 · Invasion · Non-small cell lung carcinoma

Electronic supplementary material The online version of this article (doi:10.1007/s10637-017-0494-4) contains supplementary material, which is available to authorized users.

✉ Tijana Stankovic
tijana.andjelkovic@ibiss.bg.ac.rs

[1] Department of Neurobiology, University of Belgrade, Institute for Biological Research "Sinisa Stankovic", Bulevar Despota Stefana 142, Belgrade 11060, Serbia

[2] Department of Pharmacology, Faculty of Medicine, School of Health Sciences, University of Thessaly, Biopolis, 41110 Larissa, Greece

Introduction

Lung cancer is the leading cause of cancer-related deaths worldwide with less than 18% 5-year patient survival rate [1]. At the time of diagnosis, about 70% of lung cancer patients are already at the advanced stage with metastases [2]. Even when diagnosed at the earliest stage, most of the patients already have micro-metastases [3]. Such frequent presence of lung cancer metastases significantly affects efficiency of conventional therapies and it is a major cause of treatment failure and high mortality rate associated with lung cancer [4]. Therefore, in the era of developing personalized cancer treatments, special efforts are focused on identifying novel targeted NSCLC therapies that could also interfere with the process of metastasis [5].

Cancer cells with higher ability to metastasize are often characterized by altered expression of different marker proteins involved in adhesion, migration and invasion, such as CXCR4, FAK, and their related signaling molecules [6]. Chemokine receptor, CXCR4, is highly overexpressed in NSCLC and plays an important role in its pathogenesis, as well as in metastasis [7, 8]. CXCR4 exerts its biological effects, at least partially, by activating downstream phosphorylation of FAK, one of the key molecules in regulating cell

Published online: 22 July 2017

adhesion and motility [9, 10]. Expression of both CXCR4 and FAK is negatively regulated by p53 and PTEN tumor suppressors [11–14]. Apart from being among the most frequently mutated genes in NSCLC [15], these two tumor suppressors have been found to be simultaneously altered in a significant number of NSCLC patients and associated with metastatic spread and dramatically shorter survival [16]. Although the individual contribution of these tumor suppressors in lung cancer metastasis is well known [17, 18], the effect of their mutual inactivation has not been elucidated so far. Here we propose that p53 and PTEN might cooperatively regulate CXCR4 and FAK expression that seems to promote an extremely metastatic phenotype and that targeting CXCR4 or FAK may be a promising strategy in suppressing the metastatic spread of p53/PTEN deficient NSCLCs.

Therefore, we first examined the invasive capacities of NCI-H460 cells where the activity of p53 and PTEN was simultaneously pharmacologically inhibited and COR-L23 cells that have intrinsically inactive both tumor suppressors (http://cancer.sanger.ac.uk/cell_lines). We further evaluated the expression of CXCR4 and FAK and their downstream signaling molecules as common targets of p53 and PTEN activity and finally, tested the ability of CXCR4 and FAK inhibitors to suppress the migratory and invasive capacities of NSCLC cells, in vitro and in vivo. Our data showed that joint inactivation of p53 and PTEN in NSCLC cells resulted in an extremely invasive phenotype. The obtained results suggest, under the experimental conditions tested herein, that CXCR4 and FAK inhibitors could be a valuable targeted therapy towards inhibiting migration and invasion of p53/PTEN deficient NSCLCs.

Materials and methods

Cells and cell cultures

NCI-H460 and COR-L23 cell lines were purchased from the American Type Culture Collection (ATCC, Rockville, MD) and European Collection of Cell Cultures (ECACC, Salisbury, UK), respectively. All the cells were maintained in RPMI 1640, supplemented with 10% FBS, 2 mM L-glutamine, 4.5 g/l glucose, 10,000 U/ml penicillin, 10 mg/ml streptomycin, 25 μg/ml amphotericin B solution at 37 °C in a humidified 5% CO_2 atmosphere.

Drugs and treatments

CXCR4 antagonist WZ811, FAK inhibitor PF-573228 and p53 inhibitor Pifitrin-α (PFT-α) were obtained from Selleckchem (Houston, Texas, USA). PTEN inhibitor, bpV(HOpic), was purchased from Santa Cruz Biotechnology (Dallas, USA). All inhibitors were disolved in DMSO (Sigma-Aldrich Chemie Gmbh, Germany) to 10 mM stocks and stored at −20 °C. Before treatment, all drugs were freshly diluted in sterile water.

To achieve individual or simultaneous inactivation of p53 and PTEN tumor suppressors, NCI-H60 cells were treated with 10 μM PFT-α and 2.5 μM bpV(HOpic), alone and in combination, for 24 h. Drugs were administered 24 h after cell seeding. Cells treated with PFT-α and bpV(HOpic), alone and in combination, from here on are designated as NCI-H460^{p53-}, NCI-H460^{PTEN-} and NCI-H460$^{p53-/PTEN-}$ cells, respectively.

To evaluate the effects of FAK and CXCR4 inhibitors, NCI-H460$^{p53-/PTEN-}$ and COR-L23 cells were treated with 1 μM PF-573228 and 1 μM WZ811 for 24 h. In NCI-H460$^{p53-/PTEN-}$ cells these treatments were administrated 2 h after the co-treatments with p53 and PTEN inhibitors.

RNA extraction and reverse transcription reaction

Total RNA was isolated using Trizol® reagent (Invitrogen Life Technologies, USA) according to the manufacturer's instructions. RNA was quantified by spectrophotometry and quality was determined by agarose gel electrophoresis. Reverse transcription reactions were performed using 2 μg of total RNA, with a High-capacity cDNA reverse transcription kit (Applied Biosystems, USA), following the manufacturers' instructions.

Quantitative real-time PCR

Quantitative real time PCR (qPCR) was used to analyze the differences in *CXCR4, FAK* and *PTEN* gene expression level. Reactions were performed by Maxima SYBR Green/ROX qPCR Master Mix (Thermo Scientific, USA) on an ABI PRISM 7000 Sequence Detection System (Applied Biosystems, USA) according to the manufacturer's recommendations, using 100 ng cDNAs and primers specific for each gene and *ACTB* as internal control for normalization [19–22]. Each sample was tested in triplicate and relative gene expression was analyzed by $2^{-\Delta\Delta Ct}$ method [23].

Flow cytometric analysis

CXCR4 protein level was detected by flow cytometric analysis. Adherent cells were harvested by trypsinization, washed in PBS and fixed in 4% paraformaldehyde for 10 min at room temperature. Cells were then permeabilized by adding ice-cold 100% methanol for 30 min at 4 °C. After washing in PBS, cells were blocked for 1 h with 0.5% BSA in PBS. Cells were then resuspended in primary antibody (mouse anti-CXCR4; Invitrogen, 35-8800) diluted in 0.5% BSA (1:100) and incubated overnight at 4 °C. After washing in PBS, cells labeled with unconjugated primary antibody were resuspended in secondary antibody (Alexa Fluor 488 goat

anti-Mouse IgG(H+L); Invitrogen, A-11001) diluted in 0.5% BSA (1:1000) and incubated for 1 h at room temperature. Cells were subsequently washed and resuspended in 1 ml of PBS. The fluorescence intensity was measured in FL1-H channel on CyFlow Space flow cytometer and analyzed by Summit analysis software.

Western blot analysis

Western blot analysis was used to analyze the differences in pFAK, pAKT and pERK level Proteins were isolated in RIPA buffer containing complete protease and phosphatase inhibitor cocktails (Roche, Mannheim, Germany). Subsequently, 30 μg of protein per lane were separated by 10% SDS-PAGE and transferred onto PVDF membranes. The membranes were blocked in 1% bovine serum albumin in Tris- buffered saline/0.1% Tween-20 (TBST) for 1 h at room temperature and incubated overnight at 4 °C with the following primary rabbit antibodies: anti-AKT (1:1000; Santa Cruz, sc-8312), anti-pAKT (1:750; Abcam, 81283), anti-ERK (1:1000; Santa Cruz, sc-94), anti-pERK (1:1000; Santa Cruz, sc-16982), anti-FAK (1:1000; Invitrogen, 701094) and anti-pFAK (pY397) (1:1000; Invitrogen, 44-625G). After several rinses in TBST, the membranes were incubated for 1 h/RT with a Horse Radish Peroxidase (HRP)-conjugated bovine anti-rabbit secondary antibody (1:5000; Abcam, 97051). Immunoreactivity was detected by enhanced chemiluminiscence (ECL, GE Healthcare) and exposed to film (Kodak Biomax). Each blot was re-probed with a primary mouse β-actin (1:5000; Santa Cruz, sc-8432) and GAPDH (1/5000; Biolegend, 649202) antibody and incubated with an anti-mouse secondary antibody (1:10,000; Cell Signaling, 7076S). All antibodies were diluted in TBST. Signals were quantified by densitometry using Image Quant software (v. 5.2, GE Healthcare) and expressed as relative values (i.e., density ratio normalized to the corresponding internal control, β-actin or GAPDH signal).

Wound healing assay

In order to evaluate the migratory potential cells were seeded in 24-well plates and grown for 24 h. Upon reaching confluence, a uniform wound was scratched into a monolayer of each well with a sterile plastic 200 μl micropipette tip. After wounding, tissue culture medium was replaced and described treatments were applied. Wound closure was monitored by imaging cells at 2× magnification on a Leica microscope (Leica Microsystems GmbH, Wetzlar, Germany) immediately and 24 h after wounding. The captured images were analyzed by ImageJ software (NIH, USA) to measure the degree of closure of the wounded area. Independent experiments were performed at least three times.

Gelatin degradation assay

To compare the ability of cells to degrade gelatin cells were seeded in 6-well plates with glass coverslips coated with AlexaFluor488 labeled gelatin (Gelatin From Pig Skin, Oregon Green® 488 Conjugate, Life Technologies, USA) at a density of 50,000 cells/well. After 24 h treatments, the cells were fixed with 4% paraformaldehyde and stained with Hoechst 33342 (Sigma-Aldrich Chemie Gmbh, Germany) and ActinRed 555 (Life Technologies, USA) for 1 h at room temperature. Cells and matching degraded gelatin areas were analyzed at 20× magnification under a Zeiss Axiovert inverted fluorescent microscope (Carl Zeiss Foundation, Germany) equipped with AxioVision 4.8 Software. The volume of the dark areas caused by gelatin degradation was measured using ImageJ software and normalized to the volume of the cell. At least 100 cells were analyzed per experiment. All experiments were performed at least three times.

Invasion assay

Next, to study the invasive capacity we used Transwell inserts (membrane pore size, 8 μm; diameter, 6.4 mm; BD Biosciences Discovery Labware) placed in 24-well plates. 200,000 cells were seeded in serum free medium in the upper chambers covered with a layer of Matrigel Basement Membrane Matrix (BD Biosciences) (500 g/ml). The lower chambers were filled with RPMI-1640 medium supplemented with 10% FBS as chemoattractant. A control sample without 10% FBS, as a measurement of spontaneous cell invasion, was included in each experiment. After the incubation, cells that invaded through the Matrigel and its underlying membrane were fixed in 4% paraformaldehyde-PBS and stained with Hoechst 33342. The cells that failed to invade remained on the upper surface and were carefully removed with a cotton swab, whereas the cells on the lower surface of the membranes were counted under a Zeiss Axiovert inverted fluorescent microscope at a 10× magnification. The average number of cells in 30 independent fields per membrane was analyzed. At least 3 independent experiments were performed. The results are presented as percentage of cells that invaded through the matrigel-coated membrane compared to the untreated control.

In vivo tumorigenicity assays

Eight weeks old NOD.Cg-*Prkdc*^{scid}*Il2rg*^{tm1Wjl}/SzJ (NSG) mice and 8–10 week-old SCID (Severe Combined Immunodeficiency) mice were used for in vivo experiments. All animal procedures were in compliance with Directive (2010/63/EU) on the protection of animals used for experimental and other scientific purposes and were approved by

the IACUC and the local Directorate-General for Regional Rural Economy and Veterinary (Lisence No 5542/228006). All mice were housed under pathogen-free conditions in the animal facility in a controlled environment (12 h dark/light cycles), fed with standard laboratory chow, and given autoclaved water.

For the in vivo tumorigenicity assays, subcutaneous injections were performed in each axillary region of the rear flanks. On the day of inoculation, NCI-H460 and COR-L23 cells were counted and diluted in 100 μl RPMI medium. Two different inoculation densities (100,000 and 10,000 cells) for both cell lines were used in NSG mice to evaluate their tumorigenic potential. Formation of palpable tumors was monitored over time. To investigate the growth rate of NCI-H460 and COR-L23 cells derived xenografts 10^6 cells of each cell line were injected in SCID mice. Mice were monitored three times a week for tumor growth. Tumor size was measured with a caliper and tumor volume was calculated using the formula V (mm3) = a × b^2/2, where V (mm3) is the tumor volume in mm3, a = length and b = width of the tumors. Each group in both types of in vivo experiments consisted of 3 mice, with 2 inocula per mice. The experiments were terminated when the tumor size reached a volume of 1500 mm^3 (about 11% of the mouse weight).

Orthotopic metastatic xenograft model

The model was established following the procedure described by Kraus-Berthier et al. [24]. Briefly, animals were anesthetized with Ketamin (Imalgene 1000, Merial) at 10 mg/kg and Xylazin (Sedaxylan, EuroVet) at 2 mg/kg, administered i.p. On the day of inoculation, NCI-H460 and COR-L23 cells were counted and diluted in 100 μl RPMI medium. NCI-H460 and COR-L23 cells were implanted at 1 × 10^6 and 5 × 10^5 inoculation densities through the chest wall into the left pleural space of SCID mice (i.pl.) in a volume of 100 μl using a 26 gauge needle. Each group consisted of 5 mice. One mouse from each group was sacrificed on day 14 to evaluate metastatic spread of NCI-H460 and COR-L23 derived tumors.

In vivo antitumor activity

Vehicle control and both inhibitors, PF-573228 and WZ811, diluted in WFI (water for injection) with 10% DMSO and 5% Tween 80, were administered i.p. 5 days in a row to NCI-H460- and COR-L23-bearing mice, starting 7 days after cell inoculation. Each treated group consisted of 4 mice, and control groups consisted of 7 mice. Animal mortality was checked daily, and the antitumor activity was evaluated comparing survival times.

Statistical analysis

Statistical analyses were performed by GraphPad Prism 6. The data obtained by qRT-PCR, wound healing, invasion tests, Western blotting and in vivo experiments were analyzed by Student t-test. Gelatin degradation data did not have a normal distribution, so the Wilcoxon matched-pairs signed rank test was carried out. Survival analyses were performed using Kaplan and Meier product-limit method. The log rank test was used to assess the significance of the difference between pairs of survival probabilities. The observed differences were considered statistically significant if $p < 0.05$.

Results

p53 and PTEN inhibition and functional status assessment in NSCLC cell lines

To test whether activities of p53 and PTEN tumor suppressors simultaneously influenced cell invasion, we pharmacologically inactivated p53 and PTEN in NCI-H460 cell line that is a wild type for both tumor suppressors (http://cancer.sanger.ac.uk/cell_lines). We used the well-known inhibitor of p53 (Pifitrin-α, PFT-α) in a 10 μM concentration previously shown to be efficient in NCI-H460 cells [25]. The efficacy of PTEN inhibitor (bpV(HOpic)) was determined by analyzing the level of pAKT in NCI-H460 cells treated with 1 μM and 2.5 μM bpV(HOpic). Western blot analyses have shown that 2.5 μM bpV(HOpic) successfully inhibited activity of PTEN by increasing AKT phosphorylation 1.7 fold compared to untreated NCI-H460 cells (Fig. 1a; $p = 0.02$). Combined treatment with 10 μM PFT-α and 2.5 μM bpV(HOpic) did not have anti-proliferative effect on NCI-H460 cells, as shown in Online Resource 1a.

Additionally, we used COR-L23 cell line with intrinsically mutated and inactivated p53 (http://cancer.sanger.ac.uk/cell_lines). By comparing *PTEN* gene expression level between COR-L23 and NCI-H460 cells using qRT-PCR, we demonstrated that COR-L23 cells have innately suppressed PTEN function. Namely, COR-L23 cells showed 11.5-fold decreased expression of *PTEN* compared to NCI-H460 cells (Fig. 1b; $p = 0.0002$). Such difference in *PTEN* expression between these two cell lines affected the level of pAKT protein as assessed by Western blot analysis. The level of pAKT in COR-L23 cells was increased 6.8 fold compared to NCI-H460 cells (Fig. 1c; $p = 0.0003$).

Increased invasive potential of NSCLC cell lines with mutually inactivated p53 and PTEN

To examine whether the simultaneous inhibition of p53 and PTEN influenced invasive capacity of NCI-H460

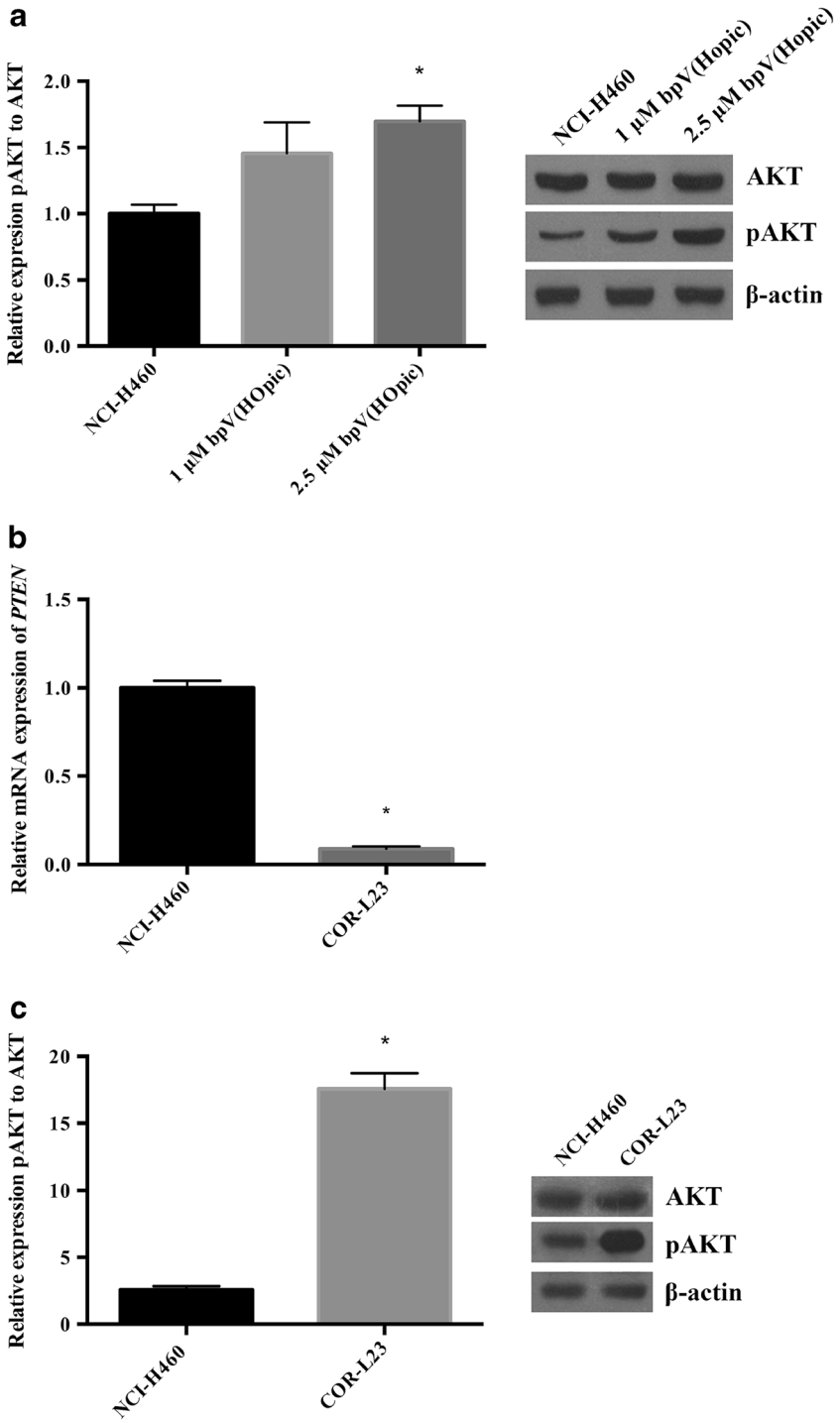

Fig. 1 PTEN inhibition and functional status assessment in NSCLC cell lines. **a** Quantification of pAKT level by Western blotting in NCI-H460 cells treated with 1 μM and 2.5 μM bpV(HOpic). **b** Quantitative real-time PCR analyses of *PTEN* gene expression in COR-L23 cells compared to NCI-H460 cells. The expression of target gene was normalized to the *ACTB* gene as internal control and is presented as a relative value compared to NCI-H460 cells. All results represent mean values ± S.E. * indicates significantly different level compared to untreated NCI-H460 cells. **c** Quantification of pAKT level by Western blotting in COR-L23 cells compared to NCI-H460 cells. The data from Western blotting experiments are expressed as the level of phospho-protein relative to total protein level, all normalized to β-actin, from at least three independent experiments and are presented as mean value ± S.E. Each graph is accompanied by representative Western blots. * indicates $p < 0.05$ compared to control NCI-H460 cells

cells, we analyzed migration and invasion of these cells treated with 10 μM PFT-α and 2.5 μM bpV(HOpic), alone (NCI-H460^{p53-} and NCI-H460^{PTEN-} cells, respectively) and in combination (NCI-H460$^{p53-/PTEN-}$ cells) using wound healing, invasion and gelatin degradation assays. Specifically, only combined treatment with PFT-α and bpV(HOpic) significantly increased cell migration in the wound healing assay 1.4-fold (Fig. 2a; $p = 0.0052$) compared to untreated cells. In invasion and gelatin degradation assays, we observed greater capacity of NCI-H460 cells to invade matrigel (Fig. 2b; 1.7-fold; $p = 0.0043$) and degrade gelatin (Fig. 2c; 1.9-fold; $p = 0.0003$) after functional inhibition of p53 and PTEN.

Moreover, COR-L23 cells with mutated p53 and significantly lower expression of PTEN showed a similar pattern of migration and invasion to NCI-H460 cells with these two

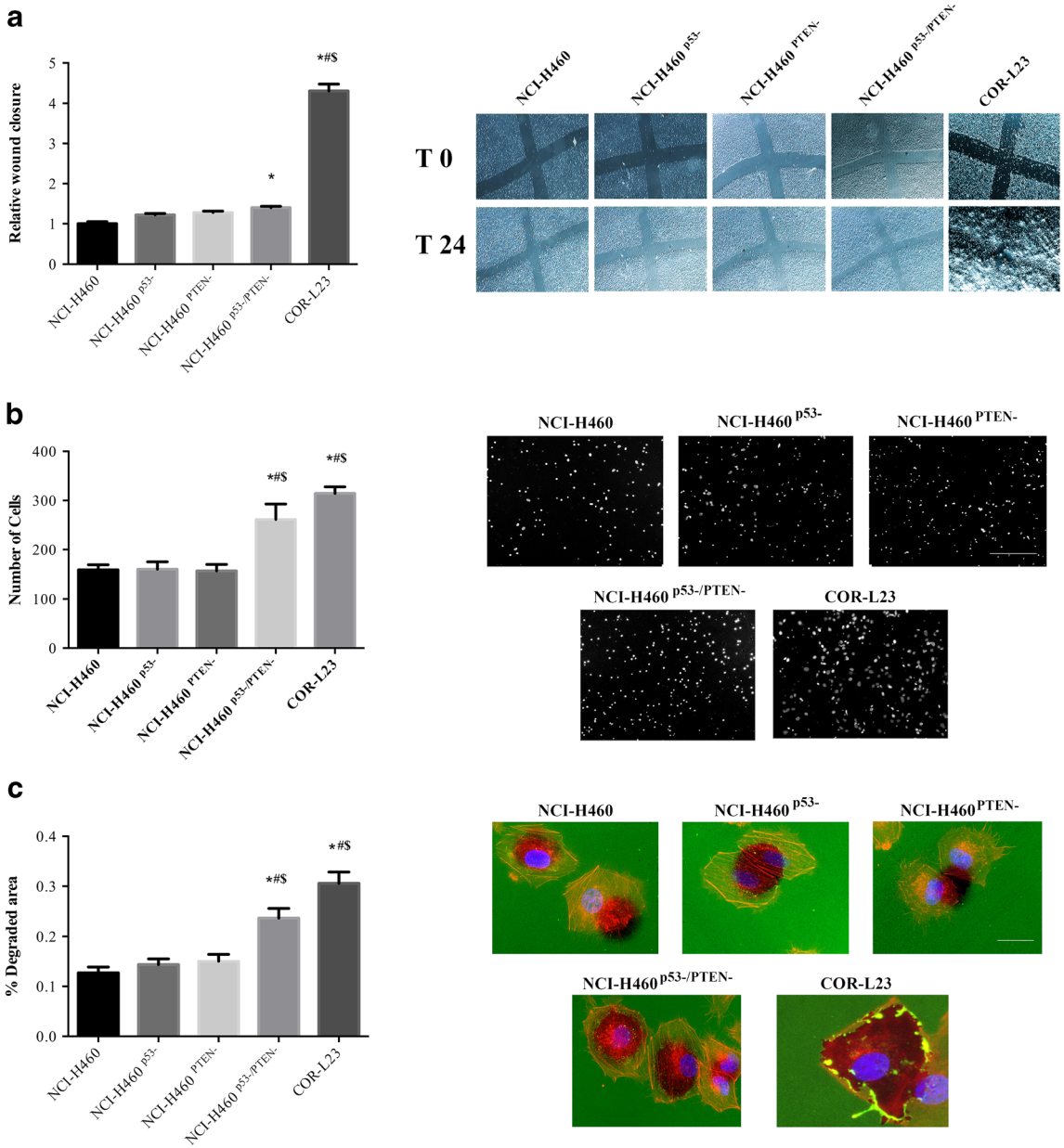

Fig. 2 Invasive potential of NSCLC cell lines with inactivated p53 and PTEN. **a** Wound healing assay of NCI-H460, NCI-H460^{p53-}, NCI-H460^{PTEN-}, NCI-H460$^{p53-/PTEN-}$ and COR-L23 cells. Histograms for each cell type showing relative wound closure compared to NCI-H460 cells are presented along with representative images, taken immediately (T 0) and 24 h (T 24) after wounding. **b** Invasion of NCI-H460, NCI-H460^{p53-}, NCI-H460^{PTEN-}, NCI-H460$^{p53-/PTEN-}$ and COR-L23 cells. Histograms for each cell type are presented along with representative images showing Hoescht 33342 stained nuclei of cells that invaded through the Matrigel to the opposite side of the membrane. Scale bar = 500 μm. **c** Gelatin degradation by NCI-H460, NCI-H460^{p53-}, NCI-H460^{PTEN-}, NCI-H460$^{p53-/PTEN-}$ and COR-L23 cells. Histograms showing percentages of degraded gelatin areas relative to the cell volume for each cell line are presented together with representative images. Merged channels show fluorescent gelatin (*green*), actin (*red*) and nuclei (*blue*) staining; dark areas represent spots of degraded gelatin. Scale bar = 100 μm. For all histograms each bar represents mean value ± S.E. * indicates $p < 0.05$ compared to NCI-H460 cells, # indicates $p < 0.05$ compared to NCI-H460^{p53-}, $ indicates $p < 0.05$ compared to NCI-H460$^{p53-/PTEN-}$ cells

tumor suppressors simultaneously inhibited (Fig. 2). More precisely, COR-L23 cells migrated at 4 times higher rate than untreated NCI-H460 cells (Fig. 2a; $p = 0.0005$), exhibited a 2-fold increase in invasion through matrigel (Fig. 2b; $p = 0.0022$) and had a 2.4-fold increase in degradation of gelatin (Fig. 2c; $p = 0.0001$).

Importantly, NCI-H460$^{p53-/PTEN-}$ and COR-L23 cells, both with dual p53 and PTEN inactivation, had also significantly increased invasion and gelatin degradation compared to NCI-H460 cells with individually inhibited p53 and PTEN, as pointed out in Fig. 2b and c. This was also true for the migratory capacity of COR-L23 cells (Fig. 2a).

Increased expression of CXCR4, FAK, AKT and ERK in NSCLC cell lines with mutually inactivated p53 and PTEN

Next, we investigated the expression level of CXCR4 and FAK, and other downstream signaling molecules, such as AKT and ERK, upon functional inhibition of p53 and PTEN. We analyzed their expression by qRT-PCR and Western blot analyses in NCI-H460 cells treated with 10 μM PFT-α and 2.5 μM bpV(HOpic), alone and in combination, as well as in COR-L23 cells. Specifically, CXCR4 protein level was quantified by flow cytometry. We found that NCI-H460^{p53-} and NCI-H460$^{p53-/PTEN-}$ cells had significantly increased expression of *CXCR4* mRNA 1.8-fold (Fig. 3a; $p = 0.047$) and 2-fold (Fig. 3a; $p = 0.022$), compared to untreated cells, respectively. In contrast, the *FAK* mRNA expression level remained unchanged upon all treatments in NCI-H460 cell line (Fig. 3b). COR-L23 cells had significantly increased expression of *CXCR4* and *FAK* mRNAs compared to NCI-H460 cells 3.1-fold (Fig. 3a; $p = 0.008$) and 1.7-fold (Fig. 3b; $p = 0.01$), respectively. On protein level, simultaneous functional inhibition of p53 and PTEN in NCI-H460 cells significantly increased CXCR4 level 2.7 fold (Fig. 4a; $p = 0.0046$) and induced FAK activation 1.7-fold (Fig. 4b; $p = 0.007$). In addition, we found that functional inhibition of p53 and PTEN in NCI-H460 cells, alone and in combination, led to significant changes in the level of pAKT compared to untreated NCI-H460 cells (Fig. 4c). More precisely, NCI-H460^{p53-} and NCI-H460^{PTEN-} cells showed significant increase in AKT phosphorylation 1.7 fold ($p = 0.003$) and 1.7-fold ($p = 0.004$) compared to NCI-H460 cells, respectively. Most importantly, NCI-H460$^{p53-/PTEN-}$ cells had the most pronounced effect on the AKT phosphorylation with 3-fold increase compared to NCI-H460 cells (Fig. 4c; $p = 0.001$). pERK level was changed only in NCI-H460$^{p53-/PTEN-}$ cells exhibiting 2.7-fold increase compared to untreated NCI-H460 cells (Fig. 4d; $p = 0.042$).

Level of CXCR4 and activation of FAK, AKT and ERK was significantly increased in COR-L23 compared to NCI-H460 cells 5.2 fold (Fig. 4a; $p = 0.001$), 2.1-fold (Fig. 4b; $p = 0.015$), 6.8-fold (Fig. 4c; $p = 0.002$) and 3-fold (Fig. 4d; $p = 0.037$), respectively.

FAK and CXCR4 inhibitors suppressed invasiveness of NSCLC cell lines with inactivated p53 and PTEN tumor suppressors

To evaluate whether NSCLC cells with mutual inactivation of p53 and PTEN (NCI-H460 $^{p53-/PTEN-}$ and COR-L23) could be responsive to FAK and CXCR4 inhibition, cells were treated with PF-573228 (FAK inhibitor) and WZ811 (CXCR4 inhibitor) and the changes in their invasive properties were analyzed. Both inhibitors, used in 1 μM concentrations, did not have considerable anti-proliferative effects on NCI-H460 $^{p53-/PTEN-}$ and COR-L23 cells (Online Resource 1b and c). In wound healing assay, we observed that NCI-H460 $^{p53-/PTEN-}$ cells treated with 1 μM PF-573228 and 1 μM WZ811, migrated at 1.34-fold ($p = 0.001$) and 1.42-fold ($p = 0.001$) slower rate, respectively, compared to untreated NCI-H460 $^{p53-/PTEN-}$ cells (Fig. 5a). More pronounced effects of the treatments were observed in invasion and gelatin degradation assays. NCI-H460 $^{p53-/PTEN-}$cells treated with PF-573228 and WZ811 had a significantly decreased invasion capacity, 4.7 (Fig. 5b; $p = 0.0002$) and 6.2 (Fig. 5b; $p = 0.0001$) fold, respectively. In addition, NCI-H460 $^{p53-/PTEN-}$ cells treated with PF-573228 and WZ811 degraded gelatin significantly

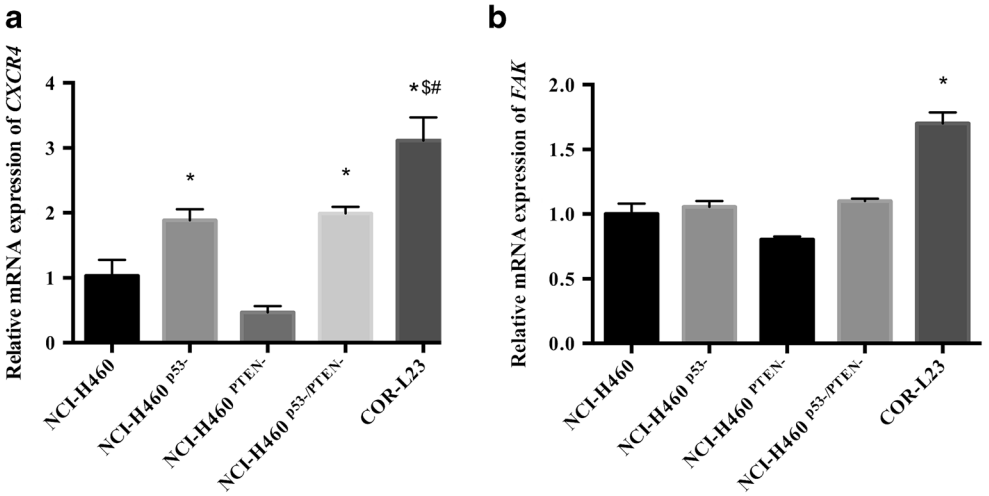

Fig. 3 Quantitative real-time PCR analyses of **a** *CXCR4* and **b** *FAK* genes expression in NCI-H460, NCI-H460^{p53-}, NCI-H460^{PTEN-}, NCI-H460$^{p53-/PTEN-}$ and COR-L23 cells. The expression of target genes was normalized to the *ACTB* as internal control and is presented as a relative value compared to NCI-H460 cells. All results are presented as mean value ± S.E. * indicates $p < 0.05$ compared to NCI-H460 cells, # indicates $p < 0.05$ compared to NCI-H460^{p53-}, $ indicates $p < 0.05$ compared to NCI-H460$^{p53-/PTEN-}$ cells

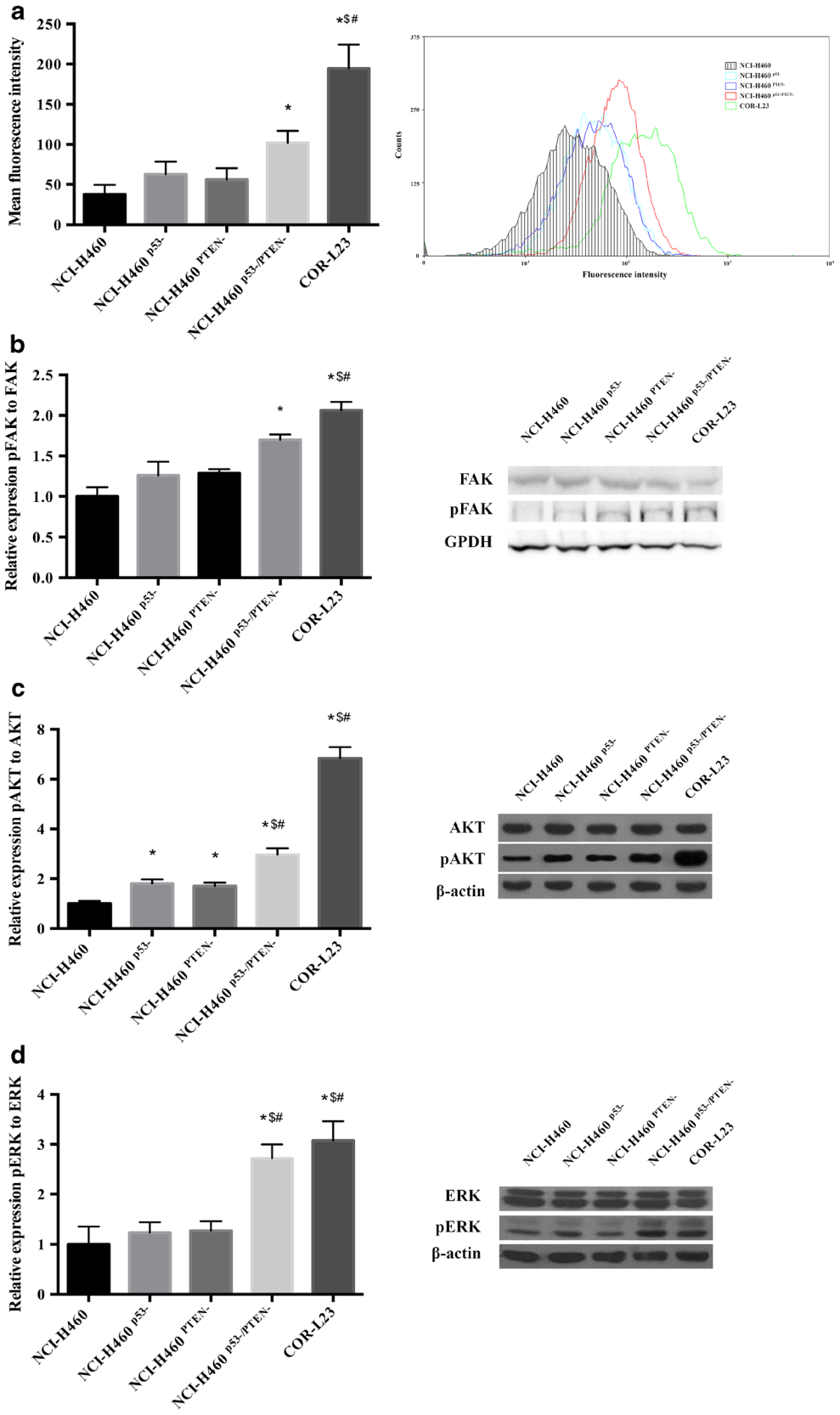

less compared to untreated cells, 5.8 (Fig. 5c; $p = 0.0001$) and 5.1 (Fig. 5c; $p = 0.0001$) fold, respectively.

The invasive behavior of COR-L23 cells upon PF-573228 and WZ811 treatments was similar to that observed in NCI-

◀ **Fig. 4** Expression analyses of CXCR4, FAK, AKT and ERK in NSCLC cell lines with inactivated p53 and PTEN. Quantification of (**a**) CXCR4 level by flow cytometry and (**b**) pFAK, (**c**) pAKT and (**d**) pERK level by Western blotting in NCI-H460, NCI-H460^{p53-}, NCI-H460^{PTEN-}, NCI-H460$^{p53-/PTEN-}$ and COR-L23 cells. The quantification and statistical analysis of flow-cytometric measurements are presented on the left part of the panel (**a**). A minimum of 10,000 events were collected for each sample. At least three independent experiments were performed. Plots of the representative experiments for each cell line are presented on the right side of the panel. The Western blot data are expressed as level of phosphoprotein relative to the total protein level, all normalized to β-actin or GAPDH. Each graph is accompanied by representative Western blots. All results are presented as mean value ± S.E. * indicates $p < 0.05$ compared to NCI-H460 cells, # indicates $p < 0.05$ compared to NCI-H460^{p53-}, $ indicates $p < 0.05$ compared to NCI-H460$^{p53-/PTEN-}$ cells

H460 $^{p53-/PTEN-}$ cells treated with FAK and CXCR4 inhibitors. According to wound healing assay, COR-L23 cells treated with 1 μM PF-573228 migrated at 1.6 times slower rate than untreated cells (Fig. 5d; $p = 0.037$), while COR-L23 cells treated with 1 μM PF-573228 and 1 μM WZ811 exhibited 2.8-fold (Fig. 5e; $p = 0.0001$) and 2.6-fold (Fig. 5e; $p = 0.0001$) decrease in invasion, respectively. In addition, COR-L23 cells treated with 1 μM PF-573228 and 1 μM WZ811 degraded gelatin 2.2-fold (Fig. 5f; $p = 0.0001$) and 2.5-fold (Fig. 5f; $p = 0.0001$) more than untreated cells, respectively.

Downregulation of pFAK and pAKT level in NSCLC cell lines treated with FAK and CXCR4 inhibitors

To examine molecular changes after the treatments with PF-573228 and WZ811 we analyzed level of pFAK, pAKT and pERK in untreated and treated NCI-H460 $^{p53-/PTEN-}$and COR-L23 cells. NCI-H460 $^{p53-/PTEN-}$ cells treated with PF-573228 and WZ811 exhibited significant reduction in FAK phosphorylation, 2.6-fold (Fig. 6a; $p = 0.0001$) and 2.1-fold (Fig. 6a; $p = 0.0001$), respectively. In addition, both PF-573228 and WZ811 treatments, led to a 2.6-fold decrease of pAKT in NCI-H460

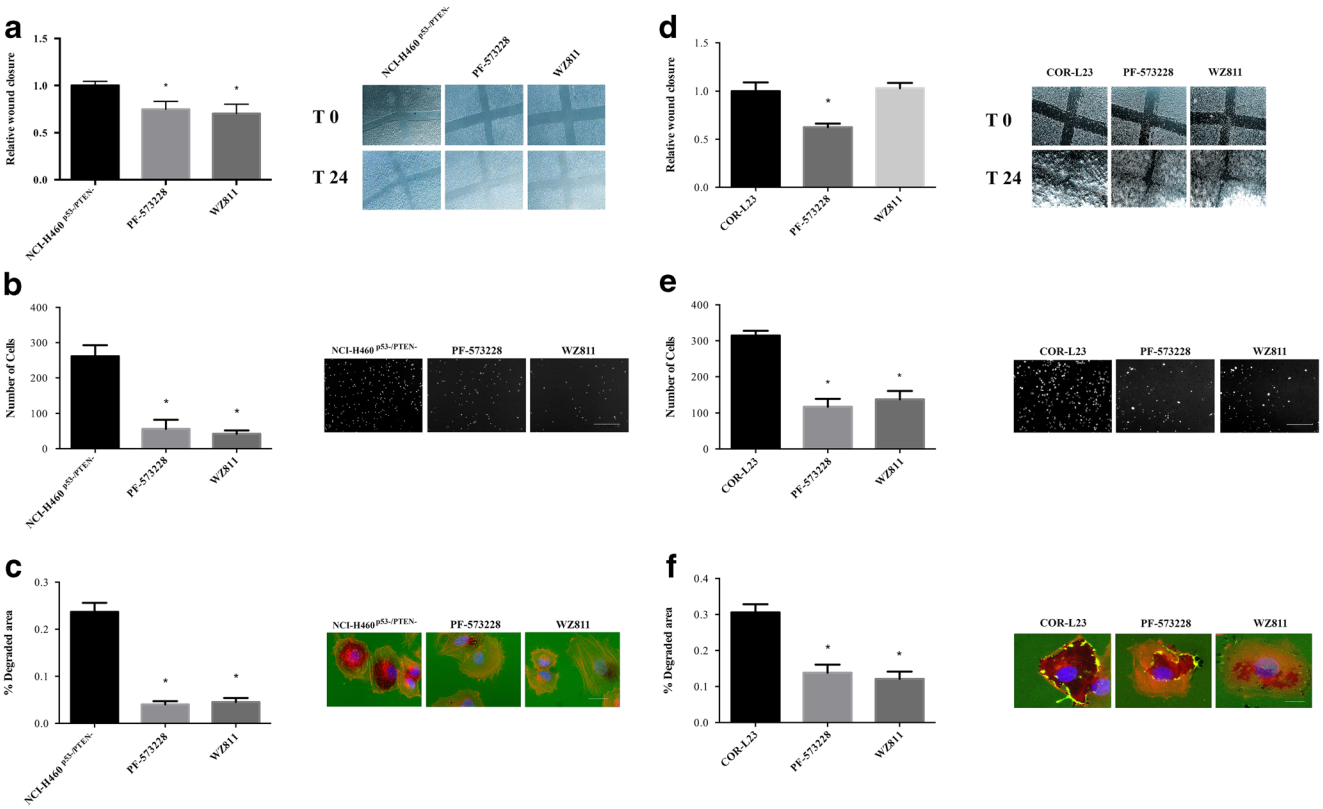

Fig. 5 Effects of FAK and CXCR4 inhibitors on invasive characteristics of NSCLC cell lines with inactivated p53 and PTEN. Wound healing assay of NCI-H460$^{p53-/PTEN-}$ (**a**) and COR-L23 (**d**) cells treated with 1 μM PF573228 and 1 μM WZ811. Histograms for each cell type showing relative wound closure compared to NCI-H460 cells are presented along with representative images, taken immediately (T 0) and 24 h (T 24) after wounding. Invasion of NCI-H460$^{p53-/PTEN-}$ (**b**) and COR-L23 (**e**) cells treated with 1 μM PF573228 and 1 μM WZ811. Histograms for each cell type are presented along with representative images showing Hoescht 33342 stained nuclei of cells that invaded through the Matrigel to the opposite side of the membrane. Scale bar = 500 μm. Gelatin degradation by NCI-H460$^{p53-/PTEN-}$ (**c**) and COR-L23 (**f**) cells treated with 1 μM PF-573228 and 1 μM WZ811. Histograms showing percentages of degraded gelatin areas relative to the cell volume for each cell line are presented together with representative images. Merged channels show fluorescent gelatin (*green*), actin (*red*) and nuclei (*blue*) staining; dark areas represent spots of degraded gelatin. Scale bar = 100 μm. For all histograms each bar represents mean value ± S.E. * indicates $p < 0.05$ compared to corresponding untreated cells, NCI-H460$^{p53-/PTEN-}$ or COR-L23 cells

$^{p53-/PTEN-}$ cells (Fig. 6b; $p = 0.0015$ and $p = 0.0008$, respectively). However, neither treatment caused pERK changes in NCI-H460 $^{p53-/PTEN-}$ cells (Fig. 6c).

COR-L23 cells treated with PF-573228 exhibited significant reduction in the phosphorylation of FAK and AKT, 2-fold ($p = 0.0018$) and 1.5-fold ($p = 0.015$), respectively, while WZ811 did not change the level of these proteins (Fig. 6d and e). The level of pERK remained unchanged upon both treatments in COR-L23 cells (Fig. 6f).

In vivo tumorigenicity, metastatic spread and anti-invasive treatment of COR-L23 derived tumors

As we have shown that cells with inactivated p53 and PTEN exhibited more aggressive phenotype responsive to anti-invasive treatments with CXCR4 and FAK inhibitors, we further aimed to verify these findings in vivo. We first developed subcutaneous lung cancer human-to-mouse xenografts to compare the tumorigenicity of NCI-H460 and COR-L23 cells. Then, we investigated the invasive and metastatic potential of both cell lines in orthotropic metastatic lung carcinoma mouse models which we further used to test anti-invasive effects of CXCR4 and FAK inhibitors.

Tumorigenicity was followed after subcutaneous inoculation of 10,000 and 100,000 of either NCI-H460 or COR-L23 cells in NOD scid gamma (NSG) mice. In these models we observed that COR-L23 tumors were developed faster in both inoculation densities as compared to NCI-H460 tumors (Table 1). More specifically, first palpable tumor was noticed in COR-L23 xenografts at day 15 following 10,000 cells'

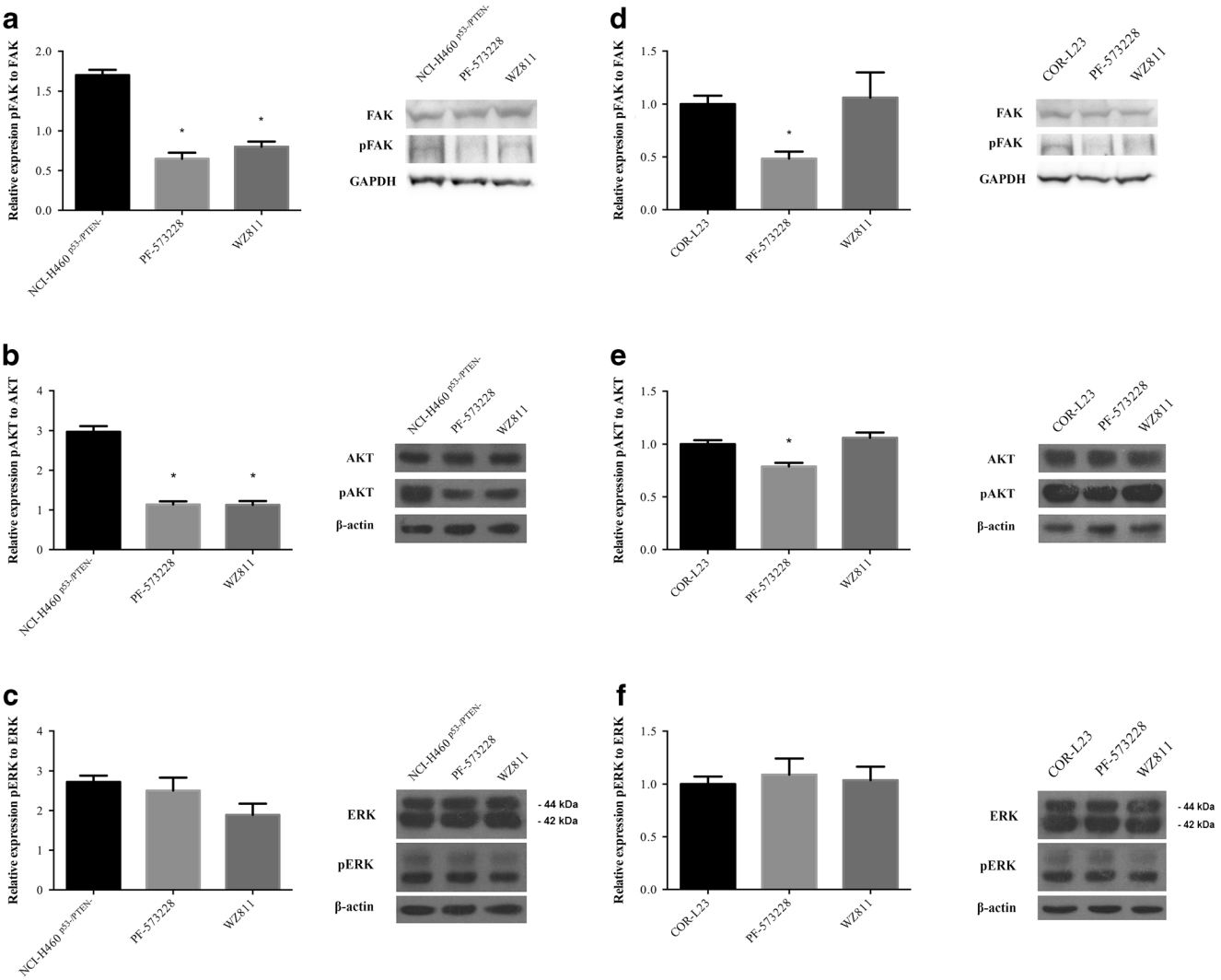

Fig. 6 Effects of FAK and CXCR4 inhibitors on protein expression of NSCLC cell lines with inactivated p53 and PTEN. Quantification of (**a**) pFAK, (**b**) pAKT and (**c**) pERK level in NCI-H460$^{p53-/PTEN-}$ cells and (**d**) pFAK, (**e**) pAKT and (**f**) pERK in COR-L23 cells after treatments with PF-573228 and WZ811. The data are expressed as the level of phospho-protein relative to total protein level, all normalized to β-actin or GAPDH, from at least three independent experiments and they are presented as mean value ± S.E. * indicates $p < 0.05$ compared to untreated cells. Each graph is accompanied by representative Western blot

Table 1 In vivo tumorigenicity assay

Day	NCI-H460	COR-L23
	Inoculation density 10,000 cells[a]	
	NoT[b] / NoI[c]	NoT / NoI
15	0 / 6	1 / 6
17	1 / 6	3 / 6
22	5 / 6	6 / 6
25	6 / 6	6 / 6
	Inoculation density 100,000 cells[a]	
	NoT / NoI	NoT / NoI
9	0 / 6	1 / 6
11	0 / 6	2 / 6
14	2 / 6	6 / 6
17	6 / 6	6 / 6

[a] In vivo tumorigenicity assay, mice were injected subcutaneously with 10,000 or 100,000 NCI-H460 and COR-L23 cells in each flank of NSG mice. Tumors formation was evaluated daily by palpation; [b] Number of tumors formed; [c] Number of inoculated tumors

inoculation, while in NCI-H460 xenografts, the first tumor was observed at day 17 post cells' inoculation. Even greater difference was observed when 100,000 cells were inoculated. COR-L23 xenografts developed the first palpable tumor at day 9, while in NCI-H460 xenografts the first palpable tumor observed at day 14 after inoculation (Table 1). Further to that, xenografts developed in SCID mice after inoculation of 10^6 cells of NCI-H460 or COR-L23 cell lines were used to evaluate tumor growth rate. Similar to the previous experiment, COR-L23 derived xenografts first formed palpable tumor, but after the 25th day NCI-H460 cells started to grow faster than COR-L23 cells and at the end of the experiment tumor derived from NCI-H460 was 1.5 volume of COR-L23 derived tumor (Fig. 7a). However, t-test analysis did not show any statistically significant difference in NCI-H460 and COR-L23 derived tumor volume.

Further, we investigated the in vivo capacity of NCI-H460 and COR-L23 cells to invade lung parenchyma. NCI-H460 and COR-L23 cells were implanted in the pleural cavity of SCID mice to obtain an orthotopic metastatic tumor model. 1×10^6 and 5×10^5 tumor cells were inoculated into the pleural space and survival time was followed. Specifically, at 1×10^6 inoculation density there was no difference in survival between NCI-H460 and COR-L23 bearing animals (data not shown). However, at 5×10^5 inoculation density, we observed a trend of shorter survival time (Fig. 7b; $p = 0.076$) in animals bearing the COR-L23 tumor, with a median survival time of 24 days for COR-L23 tumors and 28 days for NCI-H460 tumors. Moreover, at day 14, the metastatic tumor progression in the pleural cavity was very aggressive for both cell lines, but in animals bearing the COR-L23 derived tumor distant metastases were seen in peritoneal organs, such as liver, colon and pancreas (Fig. 7c).

Finally, we evaluated the potential of CXCR4 and FAK inhibitors to suppress a metastatic progression of COR-L23 derived tumor in orthotopic metastatic NSCLC model. Although no statistical analysis could be performed here due to the small group size, the results suggest that both PF-573228 and WZ811 demonstrated a trend of the life span increase in the tumor-bearing treated mice (Fig 7d). Particularly, WZ811 was found to prolong the median survival by 4 days (20% increase, median survival for treated mice 24 days as compared to a median survival of 20 days for the vehicle treated mice that served as controls).

Discussion

NSCLC represents one of the most aggressive malignant diseases characterized by frequent and extensive appearance of metastases. A number of different genes drive the metastatic spread of NSCLC, including p53 and PTEN tumor suppressors that regulate important signaling pathways involved in the cell migration and invasion [17, 18]. These two tumor suppressors are among the most commonly inactivated genes in human cancers. Individually, they have very important roles in sustaining cellular homeostasis but they are also involved in complex regulatory interactions [26]. However, their simultaneous inactivation has different implications in pathogenesis of various cancer types [27–30]. Specifically, co-inactivation of *TP53* and *PTEN* has been shown to be a significant characteristic of NSCLC patients, particularly of those with a positive lymph node invasion [16]. Nevertheless, their cooperative role in promoting the metastatic phenotype of NSCLC has not been studied so far.

To test the effects of simultaneous inactivation of p53 and PTEN tumor suppressors on invasive characteristics of NSCLC cells, we used the NCI-H460 large cell carcinoma line that expresses wild type p53 and PTEN which we subsequently pharmacologically inhibited using the well-known inhibitors PFT-α and/or bpV(HOpic), respectively. Specificity and efficacy of the applied inhibitors at used concentrations have been reported in previous publications [25, 31]. Additionally, we employed another large cell lung carcinoma cell line, COR-L23, as a model with intrinsically suppressed function of both tumor suppressors. In accordance with previously published clinical data [16], COR-L23 and p53/PTEN deficient NCI-H460 cells exhibited the most aggressive phenotype. These cells had significantly higher ability to migrate, invade and degrade gelatin compared to the wild type cells, as well as cells with individually inactivated single tumor suppressors. Similarly, a recent study on glioblastoma cell lines

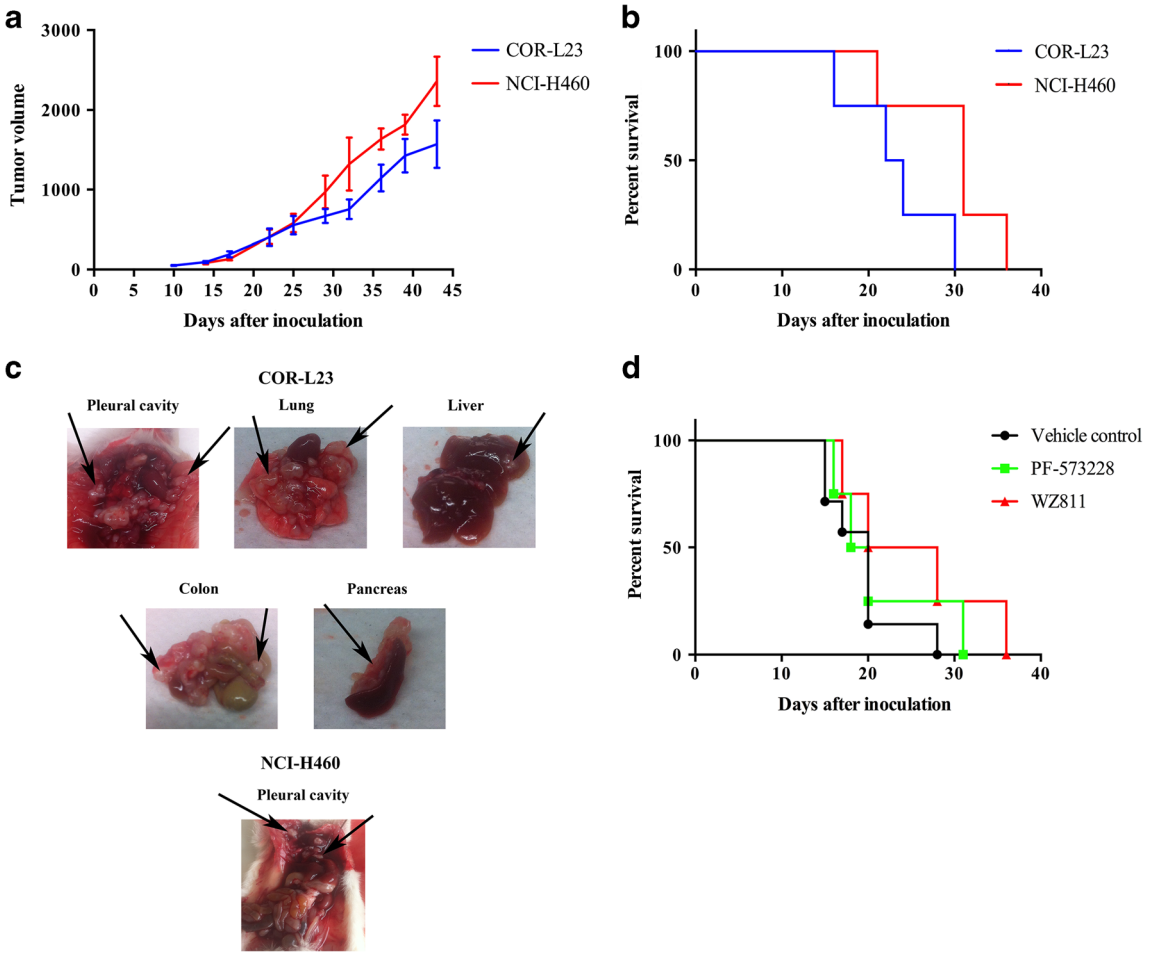

Fig. 7 In vivo tumorigenicity, metastatic spread and anti-invasive treatment of COR-L23 derived tumors. **a** Growth rate of NCI-H460 and COR-L23 derived tumors in SCID mice. **b** Survival curves of animals bearing tumors derived upon inoculation of 5×10^5 of NCI-H460 and COR-L23 cells in the pleural cavity of SCID mice. **c** Metastatic spread of COR-L23 compared to NCI-H460 derived tumors in orthotopic metastatic tumor model; *arrows* indicate tumor masses in pleural cavity and distant organs. **d** Survival curves of COR-L23 tumor-bearing mice treated with PF-573228 and WZ811, as well as vehicle control

has shown that p53/PTEN deficient cells exhibited the highest invasive potential through matrix and underlying porous membrane [32]. Moreover, p53 and PTEN were shown to have cooperative anti-invasive effects in Src-transformed vascular smooth muscle cells and fibroblasts by antagonizing Src/Stat3 pathway and repressing Src-induced podosome formation [33, 34]. In addition, our results show more pronounced invasive phenotype of COR-L23 cells compared to NCI-H460$^{p53-/PTEN-}$ cells. This could be possibly attributed to the limited efficiency of p53 and PTEN inhibition in NCI-H460 cells. Additionally, other inherent differences between the two cell lines could affect invasive capacity of COR-L23 cells.

Individually, PTEN and p53 act as negative regulators of CXCR4 and FAK expression. Namely, p53 represses transcription of both FAK and CXCR4, while PTEN dephosphorylates FAK and modulates CXCR4 expression through AKT signaling [11–14]. However, the effects of simultaneous inhibition of p53 and PTEN on CXCR4 and FAK expression and activation of their signaling pathways are poorly studied. Djuzenova and colleagues observed that glioblastoma cell lines carrying mutations in p53 or PTEN exhibited a moderately increased level of total FAK and phospho-FAK (Ser910) while the phosphorylation of FAK (Tyr397) was abolished [32]. Our results showed that *FAK* gene expression was increased in COR-L23 cells while the level of pFAK (Tyr397) was elevated in both COR-L23 and NCI-H460 cells with functionally inhibited p53 and PTEN. CXCR4 mRNA and protein levels were increased in both COR-L23 and NCI-H460cells with co-inhibited p53 and PTEN. Finally, the activity of downstream signaling molecules, pAKT and pERK, was increased in both cell lines with inactive p53 and PTEN, implying a key role of dual p53/PTEN inactivation for complete activation of CXCR4 and FAK signaling pathways. Similarly to the differences in invasive properties between the two cell lines, the levels of all investigated proteins were higher in COR-L23 cells. This could be also assigned to the incomplete

inhibition of p53 and PTEN in NCI-H460 cells, as well as other inherent differences between the two cell lines.

Consequently, targeting CXCR4 and FAK in NSCLC cells with co-inactivated p53 and PTEN was used to suppress their invasive potential. Our results demonstrated that inhibition of CXCR4 and FAK with respective inhibitors significantly suppressed ability of NCI-H460$^{p53-/PTEN-}$ and COR-L23 cells to migrate, invade and degrade gelatin. We observed that both WZ811 and PF-573228 achieved their anti-invasive effects in NCI-H460$^{p53-/PTEN-}$ cells, at least partially, by reducing the activity of FAK and AKT. This is in accordance with the fact that CXCR4-induced migration can be mediated by PI3 kinase activation of FAK and/or AKT [8] while FAK can also function upstream of PI3K/AKT [35]. However, in COR-L23 cells only FAK inhibitor decreased level of pFAK and pAKT. The absence of any WZ811 effects on the studied proteins may suggest the involvement of other signaling pathways that need to be further elucidated. ERK pathway remained unchanged in both cell lines upon all treatments. This is in line with findings that CXCR4 signaling goes through the PI3K/Akt pathway when PTEN is inactive [36] and that FAK inhibition predominantly activates AKT rather than ERK signaling in lung cancer [37].

Several in vivo studies, on sarcoma, breast, bladder and prostate carcinomas, have shown that dual p53/PTEN suppression causes highly aggressive phenotype with pronounced metastatic behavior that leads to a significantly decreased survival [38–41]. Consequently, we extended the study to animal models of lung carcinoma, using orthotopic metastatic model of NSCLC in which we observed a tendency of decreased survival among mice with inoculated COR-L23 cells. Since NCI-H460 and COR-L23 cells did not show a statistically significant difference in regard to their tumorigenic potential in both NSG and SCID mice, shorter life span of COR-L23 tumor bearing animals could be attributed to COR-L23 tumor invasiveness and development of distant metastasis. Several targeted inhibitors, such as eEF2K and PARP/PI3K inhibitors, were successfully used to suppress growth of p53/PTEN deficient xenografts of different cancer types [41, 42]. However, our study is the first one that targeted CXCR4 and FAK in orthotopic models of p53/PTEN deficient tumors. We further observed a trend of slightly prolonged survival of animals with orthotopically inoculated COR-L23 cells upon treatments with WZ811 and PF-573228. These data suggest that CXCR4 and FAK can be useful as targets to suppress the aggressiveness of p53/PTEN deficient tumors. However, the lack of an appropriate statistical analysis in these experiments implies a need for a much more detailed evaluation of other CXCR4 and FAK inhibitors with better bioavailability, and possibly alternative methods of administration.

Overall, our study demonstrated that p53/PTEN deficient NSCLC cells have particularly invasive phenotype associated with hyperactivation of CXCR4 and FAK signaling pathways. Our results point out the importance of subclassifying NSCLC patients according to p53 and PTEN functional status and to the potential of using CXCR4 and FAK inhibition to suppress metastatic spread of particularly aggressive p53/PTEN deficient tumors.

Compliance with ethical standards

Conflict of interest The authors declare no conflict of interest.

Funding This study was supported by the Ministry of Education, Science and Technological Development of the Republic of Serbia (Grant Nos III41031 and 173020), COST Action CM1106 "Chemical Approaches to Targeting Drug Resistance in Cancer Stem Cells" and COST Action CM1407 "Challenging organic syntheses inspired by nature - from natural products chemistry to drug discovery".

Ethical approval This article does not contain any studies with human participants performed by any of the authors.

All animal procedures were in compliance with Directive (2010/63/EU) on the protection of animals used for experimental and other scientific purposes and was approved by the IACUC and the local Directorate-General for Regional Rural Economy and Veterinary (Licence No 5542/228006).

References

1. Torre LA, Siegel RL, Jemal A (2016) Lung cancer statistics. Adv Exp Med Biol 893:1–19. doi:10.1007/978-3-319-24223-1_1
2. Molina JR, Yang P, Cassivi SD, Schild SE, Adjei AA (2008) Non-small cell lung cancer: epidemiology, risk factors, treatment, and survivorship. Mayo Clin Proc 83(5):584–594. doi:10.4065/83.5.584
3. Passlick B, Izbicki JR, Kubuschok B, Nathrath W, Thetter O, Pichlmeier U, Schweiberer L, Riethmuller G, Pantel K (1994) Immunohistochemical assessment of individual tumor cells in lymph nodes of patients with non-small-cell lung cancer. J Clin Oncol Off J Am Soc Clin Oncol 12(9):1827–1832. doi:10.1200/JCO.1994.12.9.1827
4. Bauml J, Mick R, Zhang Y, Watt CD, Vachani A, Aggarwal C, Evans T, Langer C (2013) Determinants of survival in advanced non–small-cell lung cancer in the era of targeted therapies. Clin Lung Cancer 14(5):581–591. doi:10.1016/j.cllc.2013.05.002
5. Chan BA, Hughes BG (2015) Targeted therapy for non-small cell lung cancer: current standards and the promise of the future. Transl Lung Cancer Research 4(1):36–54. doi:10.3978/j.issn.2218-6751.2014.05.01
6. Ben-Baruch A (2009) Site-specific metastasis formation: chemokines as regulators of tumor cell adhesion, motility and invasion. Cell Adhes Migr 3(4):328–333
7. Phillips RJ, Burdick MD, Lutz M, Belperio JA, Keane MP, Strieter RM (2003) The stromal derived factor-1/CXCL12-CXC chemokine receptor 4 biological axis in non-small cell lung cancer metastases. Am J Respir Crit Care Med 167(12):1676–1686. doi:10.1164/rccm.200301-071OC
8. Otsuka S, Bebb G (2008) The CXCR4/SDF-1 chemokine receptor axis: a new target therapeutic for non-small cell lung cancer. J Thorac Oncol Off Publ Int Assoc Study Lung Cancer 3(12):1379–1383. doi:10.1097/JTO.0b013e31818dda9d
9. Fernandis AZ, Prasad A, Band H, Klosel R, Ganju RK (2004) Regulation of CXCR4-mediated chemotaxis and chemoinvasion

of breast cancer cells. Oncogene 23(1):157–167. doi:10.1038/sj.onc.1206910
10. Mitra SK, Hanson DA, Schlaepfer DD (2005) Focal adhesion kinase: in command and control of cell motility. Nat Rev Mol Cell Biol 6(1):56–68. doi:10.1038/nrm1549
11. Conley-LaComb MK, Saliganan A, Kandagatla P, Chen YQ, Cher ML, Chinni SR (2013) PTEN loss mediated Akt activation promotes prostate tumor growth and metastasis via CXCL12/CXCR4 signaling. Mol Cancer 12(1):85. doi:10.1186/1476-4598-12-85
12. Mehta SA, Christopherson KW, Bhat-Nakshatri P, Goulet RJ Jr, Broxmeyer HE, Kopelovich L, Nakshatri H (2007) Negative regulation of chemokine receptor CXCR4 by tumor suppressor p53 in breast cancer cells: implications of p53 mutation or isoform expression on breast cancer cell invasion. Oncogene 26(23):3329–3337. doi:10.1038/sj.onc.1210120
13. Tamura M, Gu J, Matsumoto K, Aota S, Parsons R, Yamada KM (1998) Inhibition of cell migration, spreading, and focal adhesions by tumor suppressor PTEN. Science 280(5369):1614–1617
14. Golubovskaya VM, Cance WG (2011) FAK and p53 protein interactions. Anti Cancer Agents Med Chem 11(7):617–619
15. Cooper WA, Lam DC, O'Toole SA, Minna JD (2013) Molecular biology of lung cancer. J Thorac Dis 5(Suppl 5):S479–S490. doi:10.3978/j.issn.2072-1439.2013.08.03
16. Andjelkovic T, Bankovic J, Stojsic J, Milinkovic V, Podolski-Renic A, Ruzdijic S, Tanic N (2011) Coalterations of p53 and PTEN tumor suppressor genes in non-small cell lung carcinoma patients. Transl Res J Lab Clin Med 157(1):19–28. doi:10.1016/j.trsl.2010.09.004
17. Gibbons DL, Byers LA, Kurie JM (2014) Smoking, p53 mutation, and lung cancer. Mol Cancer Res : MCR 12(1):3–13. doi:10.1158/1541-7786.MCR-13-0539
18. Perez-Ramirez C, Canadas-Garre M, Molina MA, Faus-Dader MJ, Calleja-Hernandez MA (2015) PTEN and PI3K/AKT in non-small-cell lung cancer. Pharmacogenomics 16(16):1843–1862. doi:10.2217/pgs.15.122
19. Ko BS, Chang TC, Chen CH, Liu CC, Kuo CC, Hsu C, Shen YC, Shen TL, Golubovskaya VM, Chang CC, Shyue SK, Liou JY (2010) Bortezomib suppresses focal adhesion kinase expression via interrupting nuclear factor-kappa B. Life Sci 86(5–6):199–206. doi:10.1016/j.lfs.2009.12.003
20. Dai X, Mao Z, Huang J, Xie S, Zhang H (2013) The CXCL12/CXCR4 autocrine loop increases the metastatic potential of non-small cell lung cancer in vitro. Oncol Lett 5(1):277–282. doi:10.3892/ol.2012.960
21. NicAmhlaoibh R, Heenan M, Cleary I, Touhey S, O'Loughlin C, Daly C, Nunez G, Scanlon KJ, Clynes M (1999) Altered expression of mRNAs for apoptosis-modulating proteins in a low level multidrug resistant variant of a human lung carcinoma cell line that also expresses mdr1 mRNA. Int J Cancer 82(3):368–376
22. Shen YH, Zhang L, Gan Y, Wang X, Wang J, LeMaire SA, Coselli JS, Wang XL (2006) Up-regulation of PTEN (phosphatase and tensin homolog deleted on chromosome ten) mediates p38 MAPK stress signal-induced inhibition of insulin signaling. A cross-talk between stress signaling and insulin signaling in resistin-treated human endothelial cells. J Biol Chem 281(12):7727–7736. doi:10.1074/jbc.M511105200
23. Livak KJ, Schmittgen TD (2001) Analysis of relative gene expression data using real-time quantitative PCR and the 2(-Delta Delta C(T)) method. Methods 25(4):402–408. doi:10.1006/meth.2001.1262
24. Kraus-Berthier L, Jan M, Guilbaud N, Naze M, Pierre A, Atassi G (2000) Histology and sensitivity to anticancer drugs of two human non-small cell lung carcinomas implanted in the pleural cavity of nude mice. Clin Cancer Res Off J Am Assoc Cancer Res 6(1):297–304
25. Zuco V, Zunino F (2008) Cyclic pifithrin-alpha sensitizes wild type p53 tumor cells to antimicrotubule agent-induced apoptosis. Neoplasia 10(6):587–596
26. Trotman LC, Pandolfi PP (2003) PTEN and p53: who will get the upper hand? Cancer Cell 3(2):97–99
27. Hu TH, Huang CC, Lin PR, Chang HW, Ger LP, Lin YW, Changchien CS, Lee CM, Tai MH (2003) Expression and prognostic role of tumor suppressor gene PTEN/MMAC1/TEP1 in hepatocellular carcinoma. Cancer 97(8):1929–1940. doi:10.1002/cncr.11266
28. Kurose K, Gilley K, Matsumoto S, Watson PH, Zhou XP, Eng C (2002) Frequent somatic mutations in PTEN and TP53 are mutually exclusive in the stroma of breast carcinomas. Nat Genet 32(3):355–357. doi:10.1038/ng1013
29. Oki E, Tokunaga E, Nakamura T, Ueda N, Futatsugi M, Mashino K, Yamamoto M, Watanabe M, Ikebe M, Kakeji Y, Baba H, Maehara Y (2005) Genetic mutual relationship between PTEN and p53 in gastric cancer. Cancer Lett 227(1):33–38. doi:10.1016/j.canlet.2004.12.006
30. Danielsen SA, Lind GE, Bjornslett M, Meling GI, Rognum TO, Heim S, Lothe RA (2008) Novel mutations of the suppressor gene PTEN in colorectal carcinomas stratified by microsatellite instability- and TP53 mutation- status. Hum Mutat 29(11):E252–E262. doi:10.1002/humu.20860
31. Pi W, Guo X, Su L, Xu W (2012) BMP-2 up-regulates PTEN expression and induces apoptosis of pulmonary artery smooth muscle cells under hypoxia. PLoS One 7(5):e35283. doi:10.1371/journal.pone.0035283
32. Djuzenova CS, Fiedler V, Memmel S, Katzer A, Hartmann S, Krohne G, Zimmermann H, Scholz CJ, Polat B, Flentje M, Sukhorukov VL (2015) Actin cytoskeleton organization, cell surface modification and invasion rate of 5 glioblastoma cell lines differing in PTEN and p53 status. Exp Cell Res 330(2):346–357. doi:10.1016/j.yexcr.2014.08.013
33. Poon JS, Eves R, Mak AS (2010) Both lipid- and protein-phosphatase activities of PTEN contribute to the p53-PTEN anti-invasion pathway. Cell Cycle (Georgetown, Tex) 9(22):4450–4454. doi:10.4161/cc.9.22.13936
34. Mukhopadhyay UK, Mooney P, Jia L, Eves R, Raptis L, Mak AS (2010) Doubles game: Src-Stat3 versus p53-PTEN in cellular migration and invasion. Mol Cell Biol 30(21):4980–4995. doi:10.1128/MCB.00004-10
35. Xia H, Nho RS, Kahm J, Kleidon J, Henke CA (2004) Focal adhesion kinase is upstream of phosphatidylinositol 3-kinase/Akt in regulating fibroblast survival in response to contraction of type I collagen matrices via a beta 1 integrin viability signaling pathway. J Biol Chem 279(31):33024–33034. doi:10.1074/jbc.M313265200
36. Begley LA, Kasina S, Shah RB, Macoska JA (2015) Signaling mechanisms coupled to CXCL12/CXCR4-mediated cellular proliferation are PTEN-dependent. Am J Clin Exp Urol 3(2):91–99
37. Zhang H, Shao H, Golubovskaya VM, Chen H, Cance W, Adjei AA, Dy GK (2016) Efficacy of focal adhesion kinase inhibition in non-small cell lung cancer with oncogenically activated MAPK pathways. Br J Cancer 115(2):203–211. doi:10.1038/bjc.2016.190
38. Martin P, Liu YN, Pierce R, Abou-Kheir W, Casey O, Seng V, Camacho D, Simpson RM, Kelly K (2011) Prostate epithelial Pten/TP53 loss leads to transformation of multipotential progenitors and epithelial to mesenchymal transition. Am J Pathol 179(1):422–435. doi:10.1016/j.ajpath.2011.03.035
39. Puzio-Kuter AM, Castillo-Martin M, Kinkade CW, Wang X, Shen TH, Matos T, Shen MM, Cordon-Cardo C, Abate-Shen C (2009) Inactivation of p53 and Pten promotes invasive bladder cancer. Genes Dev 23(6):675–680. doi:10.1101/gad.1772909
40. Guijarro MV, Dahiya S, Danielson LS, Segura MF, Vales-Lara FM, Menendez S, Popiolek D, Mittal K, Wei JJ, Zavadil J, Cordon-Cardo C, Pandolfi PP, Hernando E (2013) Dual Pten/Tp53

suppression promotes sarcoma progression by activating Notch signaling. Am J Pathol 182(6):2015–2027. doi:10.1016/j.ajpath.2013.02.035

41. Liu JC, Voisin V, Wang S, Wang DY, Jones RA, Datti A, Uehling D, Al-awar R, Egan SE, Bader GD, Tsao M, Mak TW, Zacksenhaus E (2014) Combined deletion of Pten and p53 in mammary epithelium accelerates triple-negative breast cancer with dependency on eEF2K. EMBO Mol Med 6(12):1542–1560. doi:10.15252/emmm.201404402

42. Gonzalez-Billalabeitia E, Seitzer N, Song SJ, Song MS, Patnaik A, Liu XS, Epping MT, Papa A, Hobbs RM, Chen M, Lunardi A, Ng C, Webster KA, Signoretti S, Loda M, Asara JM, Nardella C, Clohessy JG, Cantley LC, Pandolfi PP (2014) Vulnerabilities of PTEN-TP53-deficient prostate cancers to compound PARP-PI3K inhibition. Cancer Discov 4(8):896–904. doi:10.1158/2159-8290.CD-13-0230